

Crystal and anion structure, TGA, DTA, and infrared and Raman spectra of manganese(II) nitroprusside dihydrate, $\text{Mn}[\text{Fe}(\text{CN})_5\text{NO}] \cdot 2\text{H}_2\text{O}$ ⁽¹⁾

A. Benavente,⁽²⁾ J. A de Morán,⁽²⁾ O. E. Piro,⁽³⁾ E. E. Castellano,⁽⁴⁾ and P. J. Aymonino^{(5)*}

Received September 9, 1996

The single crystal and anion structure of $\text{Mn}[\text{Fe}(\text{CN})_5\text{NO}] \cdot 2\text{H}_2\text{O}$, obtained by slow interdiffusion of reactant solutions through a TMS gel, was solved by X-ray diffraction methods and refined to $R1 = 0.036$. Spatial group: orthorhombic, $Pnma$, $a = 14.069(2)$, $b = 7.538(1)$, $c = 10.543(1)\text{Å}$, $Z = 4$. The Mn(II) ion and the water molecules are sited on mirror planes, which bisect the nitroprusside ions. One of the water molecules is coordinated to Mn(II) and the other, strongly hydrogen (as acceptor) bonded to the first molecule. The IR spectrum confirms the bonding of the water molecules and TGA results are in accordance with the dihydrate character of the substance and its dehydration in two successive steps. DTA results and the Raman spectrum agree with other results and the comparison between IR and Raman νNO wavenumbers confirms the expected strong vibrational interaction between the closely packed antiparallel (eclipsed) NO groups. There is a topotactic relationship between the dihydrate and the trihydrate, which crystallizes in the space subgroup $P2_1/n$.

KEY WORDS: Manganese nitroprusside dihydrate; crystal structure; properties.

Introduction

Bivalent transition and post-transition metal nitroprussides, $\text{M}[\text{Fe}(\text{CN})_5\text{NO}] \cdot n\text{H}_2\text{O}$ ($\text{M} = \text{Mn}, \text{Fe}, \text{Co}, \text{Ni}, \text{Cu}, \text{Zn}, \text{Cd}; n = 2-6$)¹ were described and divided

on the basis of the infrared spectra into two groups, one comprising Mn, Zn, and Cd, and the other, Fe, Co, Ni, and Cu. Manganese(II) nitroprusside ($\text{Mn}[\text{Fe}(\text{CN})_5\text{NO}] \cdot n\text{H}_2\text{O}$) was reported as a dihydrate but most recently a trihydrate, stable only in the presence of the mother liquor, was also reported.² It was also found that this higher hydrate dehydrates rapidly under atmospheric conditions to a dihydrate. The crystal structure of the trihydrate was described as belonging to the monoclinic $P2_1/n$ spatial group, $a = 7.302(4)$, $b = 14.783(6)$, $c = 10.751(1)\text{Å}$, $\beta = 91.47(2)^\circ$, $Z = 4$.²

Unable to obtain the trihydrate, the crystals grown by slow interdiffusion of solutions of the reactants, MnCl_2 or MnSO_4 and $\text{Na}_2[\text{Fe}(\text{CN})_5\text{NO}]$, through a TMS gel, and kept under mother liquor (obtained from the preparation of the salt by rapid mixing of the reactant solutions), showed to be the dihydrate.

The crystal structure of the dihydrate belongs to the orthorhombic $Pnma$ space group No. 62. Its FTIR (for its dispersive IR spectra see ref. 1) and FTNIRR spectra are discussed taking advantage of the new crys-

⁽¹⁾ Dedicated to Prof. Dr. A. Müller, Bielefeld, Germany, in occasion of his 60th anniversary.

⁽²⁾ Instituto de Química Inorgánica, Facultad de Bioquímica, Química y Farmacia, Universidad Nacional de Tucumán, Argentina.

⁽³⁾ Laboratorio Nacional de Difracción de Rayos X (LANADI) and Programa PROFIMO (CONICET-UNLP), Departamento de Física, Facultad de Ciencias Exactas, Universidad Nacional de La Plata, Argentina.

⁽⁴⁾ Instituto de Física e Química de São Carlos, Universidade de São Paulo, C. P. 369, 13560 São Carlos, Brasil.

⁽⁵⁾ Centro de Química Inorgánica (CEQUINOR) (CONICET-UNLP) and Laboratorio Nacional de Espectrofotometría Óptica LANAIS EFO (CONICET-UNLP), Departamento de Química, Facultad de Ciencias Exactas, Universidad Nacional de La Plata, C. C. 962, 1900 La Plata, Argentina.

* To whom correspondence should be addressed.

tallographic knowledge. The νNO wavenumbers obtained in the two types of spectra are compared in order to confirm the strong vibrational interaction between close-packed and antiparallel NO groups expected from crystallographic results.

There is a topotactic relationship between the trihydrate and the dihydrate, a case comparable to the system: $\text{Sr}[\text{Fe}(\text{CN})_5\text{NO}] \cdot 4\text{H}_2\text{O} - \text{Sr}[\text{Fe}(\text{CN})_5\text{NO}] \cdot 2\text{H}_2\text{O}$. Years ago we were able to dehydrate the tetrahydrate with P_4O_{10} in a Lindemann capillary tube and to solve the intimate structure of the new crystals of the dihydrate which remained arranged into a mosaic of nearly parallel oriented crystallites keeping the external form of the original crystal of the tetrahydrate (in this case, the structural topotactic modification which took place was from $C2/m^3$ to $Ccmm$ space group).⁴ The topotactic relationship seems to extend also to the monohydrate and the anhydrate as deduced from the powder spectra of the whole series of compounds.⁵

Other nitroprussides form different hydrates, i.e. the lithium salt can be obtained as a di-,⁶ tri-, and tetrahydrate.⁷ $\text{K}_2[\text{Fe}(\text{CN})_5\text{NO}] \cdot n\text{H}_2\text{O}$ crystallizes either with $n = 1$,⁸ $n = 1.25$ (a sesquiquarter-hydrate),⁹ $n = 2$ ¹⁰ and $n = 2.5$.¹¹ Rubidium nitroprusside crystallizes either as anhydrous¹² or a monohydrate.^{7,13} Cesium nitroprusside can also be obtained as an anhydrate¹⁴ or a monohydrate.¹⁵ $\text{Ca}[\text{Fe}(\text{CN})_5\text{NO}]$ has been obtained either as a monohydrate,¹⁶ a trihydrate,⁷ or a tetrahydrate¹⁷ and $\text{Ba}[\text{Fe}(\text{CN})_5\text{NO}]$ (BaPN) crystallizes either as a trihydrate¹⁸ or hexahydrate.¹⁹

The interest in nitroprussides has recently been renewed by the discovery of what is supposed to be electronically excited metastable states of striking spectroscopic behavior in $\text{Na}_2[\text{Fe}(\text{CN})_5\text{NO}] \cdot 2\text{H}_2\text{O}$ (NaNP),²⁰⁻²² and in a whole series of nitroprusside-containing salts.²³ Other $\text{Na}_2[\text{M}(\text{CN})_5\text{NO}] \cdot 2\text{H}_2\text{O}$ salts ($\text{M} = \text{Ru}$,^{24a} Os ^{24b}) show the same behavior as the isostructural NaNP.

Nitroprusside salts are also of interest because some of them show a marked correlation splitting of the IR and Raman modes of the NO stretching of the anion due to a favorable arrangement of the NO groups (piled up at short distances from each other, antiparallel or nearly antiparallel intercalated, forming chains, well separated from each other). This is the case for BaNP in which IR and Raman spectra show the νNO band at 1947 cm^{-1} ,^{25,26} and 1936 cm^{-1} ,²⁷ respectively (see ref. 26 for the coupling treatment). $\text{Sr}[\text{Fe}(\text{CN})_5\text{NO}] \cdot 4\text{H}_2\text{O}$ also shows a strong vibrational coupling between neighboring NO groups.²⁶

$\text{Mn}[\text{Fe}(\text{CN})_5\text{NO}] \cdot 2\text{H}_2\text{O}$ should show a splitting due to a similar arrangement of the NO groups (intercalated, antiparallel, or nearly antiparallel piled up along double chains of anions) and, in fact, similar IR-Raman splitting as in the barium salt (trihydrate)²⁵⁻²⁷ has been observed.

Experimental

Preparative

$\text{Mn}[\text{Fe}(\text{CN})_5\text{NO}] \cdot 2\text{H}_2\text{O}$ (MnNP) single crystals were prepared at room temperature by slow interdiffusion of 0.1 M solutions of MnSO_4 and $\text{Na}_2[\text{Fe}(\text{CN})_5\text{NO}]$ through a TMS gel because the very low solubility of MnNP did not allow any other simpler method. The process took about three months to produce small single crystals (of a few tenths of a millimeter) suitable for X-ray diffraction measurements.

The small, elongated, red-brown prismatic crystals were separated from the gel, washed with mother liquor obtained from the reaction by direct mixing of reactants solutions and kept under the mother liquor. Other crystals were kept either under a (1:1) ethanol-water mixture or absolute ethanol, with the same result in all cases because the hydrate obtained was always the dihydrate. Crystals kept at ambient conditions proved to be the dihydrate, as suggested in ref. 2.

MnNP powder was obtained by mixing the solutions of above, filtering the solid formed, washing it with distilled water and alcohol and drying it in the atmosphere. TGA, DTA, IR, and Raman measurements were performed with the prepared powder.

TGA, DTA

TGA and DTA measurements were performed under flowing dry nitrogen (50 ml/min) between room temperature and 500°C with a heating rate of $5^\circ\text{C}/\text{min}$ on air dried samples with Shimadzu TGA 50 and DTA 50 units, respectively. The instruments were calibrated with standard weights and calcium oxalate in the TGA mode, and indium and zinc, for DTA. Temperatures are believed to be $\pm 1^\circ\text{C}$ accurate in the DTA mode.

X-ray diffraction study

X-ray diffraction data was collected with single crystals, either air-dried or sealed in the Lindemann

capillaries in the presence either of small quantities of the mother solution, a mixture of (1:1) water and ethanol or absolute ethanol. Crystal data, data collection procedure, structure determination methods and refinement of results are summarized in Table 1.

IR and Raman spectra

FTIR and FTNIRR spectra were performed with Bruker IFS66 and IFS113v instruments (belonging to the National Laboratory for Research and Services in Optical Spectrophotometry, LANAIS EFO, located at Universidad Nacional de La Plata, Argentina). IR samples were prepared in KBr or polyethylene wafers,

according to the spectral region searched. Calibration of instruments was periodically performed with atmospheric water and CO₂ bands and polystyrene bands as well. The Raman spectra were run with the FTNIRR attachment mounted on the IFS66 instrument. Samples were held in the special support for solid samples and exposed to the air. Calibration was performed with sulfur. Accuracy and reproducibility were believed to be ± 1 and ± 2 cm⁻¹ for sharp bands at the same resolutions, respectively. When necessary, band deconvolution was performed with software provided with the interferometers.

Results and discussion

TGA, DTA

Typical TGA and DTA curves are shown in Fig. 1a. The first part of the TGA curve and the corresponding derivative are presented in a larger scale in Fig. 1b to show details not seen in Fig. 1a. An endothermic TGA process begins as soon as the sample is heated and finishes at about $162 \pm 35^\circ\text{C}$. The curve shows, in detail, three inflexion points. The middle one is located at $127 \pm 3^\circ\text{C}$. Up to this point a weight loss of $5.65 \pm 0.13\%$ (expected for one water molecule: 5.87%) is registered, and after it $6.77 \pm 0.25\%$ (c.f. the loss expected for a water molecule), while total weight loss is $11.74 \pm 0.79\%$ (mean of five determinations; expected for two water molecules: 11.74%). The dihydrate nature of the sample is thus confirmed and the existence of a loosely bonded water molecule (W2) and a more tightly bonded one (W1) is strongly suggested. At higher temperatures, up to 500°C , the expected second TGA feature begins at about $290 \pm 26^\circ\text{C}$ and ends at ca. $367 \pm 12^\circ\text{C}$; weight change is $17.11 \pm 0.14\%$ (expected for the evolution of $\text{NO} + 1/2(\text{CN})_2$ 18.25%).

The DTA curve shows, at about $78 \pm 6^\circ\text{C}$, a broad endothermic shoulder followed by an endothermic broad peak located at $113 \pm 14^\circ\text{C}$. The relative heats involved in the two steps seem to be in the ratio of about 1:1.5. The dehydration process is followed by another endothermic reaction, which begins at ca. 300°C and ends at ca. 360°C with a maximum at $340 \pm 8^\circ\text{C}$.

The TGA and DTA behavior of MnNP is comparable to the deportment of other hydrated nitroprussides but not exactly as NaNP³⁰ because this substance loses water, as expected, in a single step but at a higher

Table 1. Crystal data and summary of intensity data collection and structure refinement for Mn[Fe(CN)₅NO]·2H₂O

Compound	Mn[Fe(CN) ₅ NO]·2H ₂ O
Color/shape	red/parallelepiped
Empirical formula	C ₅ H ₄ FeMnN ₆ O ₃
Formula weight	306.91
Temperature	293 K
Crystal system	Orthorhombic
Space group	<i>Pnma</i>
Unit cell dimensions	<i>a</i> = 14.069(2) Å
(25 reflections in 7.85 to	<i>b</i> = 7.538(1) Å
22.05° θ range)	<i>c</i> = 10.543(1) Å
Volume	1118.1(3) Å ³
Z	4
Density (calculated)	1.823 Mg/m ³
Absorption coefficient	2.384 mm ⁻¹
Diffractometer/scan	Enraf-Nonius CAD-4/ ω -2 θ
Radiation/wavelength	MoK α (graphite monochrom.)/ λ = 0.71069 Å
<i>F</i> (000)	604
Crystal size	0.25 mm
θ range for data collection	2 to 60°
Index ranges	$-1 \leq h \leq 19$, $-1 \leq k \leq 5$, $-1 \leq l \leq 14$
Reflections collected	1709
Independent/obs. reflects.	1248/962 ($ I > 2\sigma(I)$)
Absorption correction	Not applied
Refinement method	Full-matrix least-squares of <i>F</i> ²
Computing	SHELXL8629 SHELXL9330
Data/restraints/parameters	1248/0/88
Goodness-of-fit on <i>F</i> ²	1.141
SHELXL93 weight parameters	0.0509, 0.8444
Final <i>R</i> index [$ I > 2\sigma(I)$]	<i>R</i> 1 = 0.036
<i>R</i> indices (all data)	<i>R</i> 1 = 0.0598, <i>wR</i> 2 = 0.1103
Largest diff. peak and hole	0.89 and -0.56 eÅ ⁻³

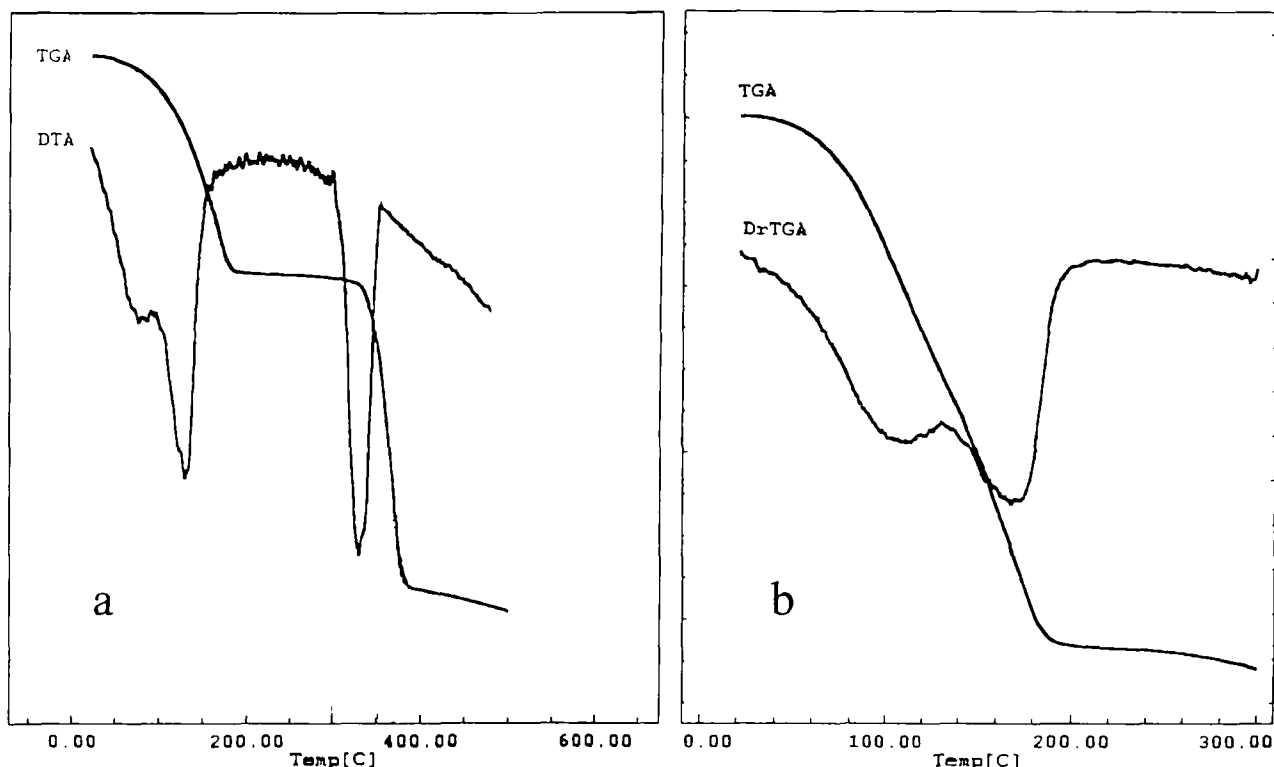


Fig. 1. (a) Typical TGA and DTA diagram of $\text{Mn}[\text{Fe}(\text{CN})_5\text{NO}] \cdot 2\text{H}_2\text{O}$; (b) enlargement of the first part of the TGA and DrTGA diagrams.

temperature than MnNP, 158°C. The decomposition of the anion in NaNP begins earlier than in MnNP, at 309°C (strong endo-DTA peak, assigned to the evolution of NO, as proved by DGE) but ends at 338°C (exo-DTA shoulder, assigned to C_2N_2), approximately the temperature of our strong endo-DTA peak.

Results obtained with MnNP handled in air confirm its dihydrate character and are in accordance with the existence of two differently bonded water molecules (see below).

Structural results

Fractional coordinates and equivalent isotropic temperature parameters according to Hamilton³¹ are given in Table 2. Bond distances and angles are in Table 3. Figure 2 is an ORTEP drawing³² of the compound with the labelling of the atoms and their vibrational ellipsoids. Figure 3 is a stereoscopic pair of a structure projection showing the crystal packing. The $[\text{Fe}(\text{CN})_5\text{NO}]$ anions, as well as the Mn^{2+} ions and the water oxygens, are sited on crystallographic mirror planes. These planes bisect the angles formed by oppo-

site pairs of adjacent equatorial cyanide ligands of the anion. The nitroprusside ion exhibits the usual distorted octahedral configuration of ligands around iron with the equatorial Fe–C bonds slightly bent towards the axial cyanide (opposite to the NO group) (Fig. 1). Fe–N, average Fe–C, N–O, and average C–N bond lengths are: 1.662(4), 1.941(8), 1.131(6),

Table 2. Fractional atomic coordinates and isotropic temperature parameters (\AA^2) of $\text{Mn}[\text{Fe}(\text{CN})_5\text{NO}] \cdot 2\text{H}_2\text{O}$

Atom	X/a	Y/b	Z/c	Beq
Fe	0.0599(0)	0.25	0.1917(1)	1.22(3)
N	0.0157(3)	0.25	0.0456(4)	1.7(1)
N(3)	0.1395(3)	0.25	0.4638(4)	2.5(2)
C(3)	0.1107(3)	0.25	0.3631(5)	1.7(2)
C(1)	-0.0263(2)	0.0670(6)	0.2533(3)	1.8(1)
C(2)	0.1539(2)	0.0690(7)	0.1591(3)	2.0(1)
N(2)	0.2087(2)	-0.0394(6)	0.1409(3)	2.5(1)
O	-0.0158(3)	0.2500(0)	-0.0531(4)	4.1(2)
N(1)	-0.0759(2)	-0.0397(6)	0.2877(3)	2.5(1)
Mn	0.1824(0)	0.25	0.6651(1)	1.33(3)
O(w1)	0.2179(4)	0.25	0.8712(4)	5.7(2)
O(w2)	0.3908(5)	0.25	0.9547(8)	9.8(4)
H(Ow1)	0.283(5)	0.25	0.903(7)	4(1)

Table 3. Interatomic bond distances (Å) and angles (°) for $\text{Mn}[\text{Fe}(\text{CN})_5\text{NO}]\cdot 2\text{H}_2\text{O}^a$

(a) Bond distances	
Fe–N	1.662(4)
Fe–C(1)	1.948(4)
Fe–C(2)	1.931(4)
Fe–C(3)	1.943(5)
N–O	1.131(6)
C(1)–N(1)	1.125(6)
C(2)–N(2)	1.140(6)
N(3)–C(3)	1.136(7)
Mn–N(1 ⁱ)	2.237(4)
Mn–N(2 ⁱⁱ)	2.221(4)
Mn–N(3)	2.207(5)
Mn–O(w1)	2.229(5)
O(w1)–O(w2)	2.587(9)
O(w1)–H(ow1)	0.97(7)
H(ow1)–O(w2)	1.61(7)
(b) Bond angles	
N–Fe–C(3)	179.6(2)
N–Fe–C(1)	94.4(2)
N–Fe–C(2)	95.2(2)
C(3)–Fe–C(1)	85.4(2)
C(3)–Fe–C(2)	85.0(2)
C(1)–Fe–C(2)	89.2(2)
C(1)–Fe–C(2 ⁱⁱⁱ)	170.4(2)
C(1)–Fe–C(1 ⁱⁱⁱ)	90.2(2)
C(2)–Fe–C(2 ⁱⁱⁱ)	89.9(2)
Fe–N–O	178.9(3)
Fe–C(1)–N(1)	179.2(4)
Fe–C(2)–N(2)	179.1(4)
Fe–C(3)–N(3)	179.2(4)
N(3)–Mn–O(w1)	177.1(1)
N(3)–Mn–N(1 ⁱ)	91.8(1)
N(3)–Mn–N(2 ⁱⁱ)	94.5(1)
O(w1)–Mn–N(1 ⁱ)	86.2(1)
O(w1)–Mn–N(2 ⁱⁱ)	87.6(1)
N(1 ⁱ)–Mn–N(2 ⁱⁱ)	88.9(1)
N(1 ⁱ)–Mn–N(2 ^{iv})	90.2(1)
N(2 ^v)–Mn–N(2 ⁱⁱ)	91.2(1)
N(1 ⁱ)–Mn–N(2 ^v)	173.7(1)
Mn–N(1 ⁱ)–C(1)	173.6(4)
Mn–N(2 ⁱⁱ)–C(2)	163.6(3)
C(3)–N(3)–Mn	75.0(3)
O(w1)–H(ow1)–O(w2)	179(1)

Symmetry code: (i) $-x, -y, 1-z$; (ii) $\frac{1}{2}-x, -y, \frac{1}{2}+z$; (iii) $x, \frac{1}{2}-y, z$; (iv) $-x, \frac{1}{2}+y, 1-z$; (v) $\frac{1}{2}-x, \frac{1}{2}+y, \frac{1}{2}+z$.

and 1.134(8) Å, respectively. Fe–N–O, average Fe–C–N, N–Fe–C_{ax}, average N–Fe–C_{eq}, trans-C_{eq}–Fe–C_{eq}, and average cis-C_{eq}–Fe–C_{eq} bond angles are 178.9(3), 179.17(6), 179.6(2), 94.8(4), 170.4(2), and 89.8(4)°, respectively. These intramolec-

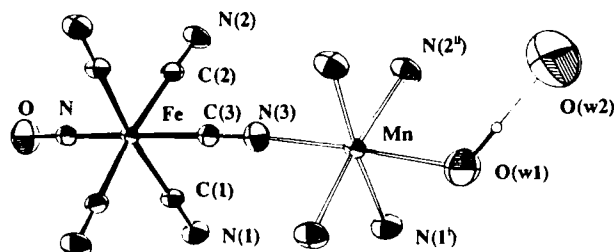


Fig. 2. ORTEP drawing of the compound with the labelling of the atoms and their vibrational ellipsoids.

ular distances and angles are in agreement with other determinations of nitroprusside geometry.⁹

The Mn(II) ion is six-fold coordinated to an axial and four equatorial nitrogen cyanides of five nitroprusside ions with an average Mn–N distance of 2.22(1) Å. The remaining ligand is a water oxygen at $d(\text{Mn}-\text{Ow1}) = 2.229(5)$ Å. Internal angles of the slightly deformed coordination octahedron are approximately 90 or 180°. W1 forms a strong linear $\text{Ow1}-\text{H}\dots\text{Ow2}$ H-bond with the other water molecule [$d(\text{Ow1}\dots\text{Ow2}) = 2.587(9)$ Å; $d(\text{H}\dots\text{Ow2}) = 1.61$ Å]. TGA–DTA findings are therefore supported by X-ray diffraction results, i.e., there are two kinds of water molecules in the structure, one more strongly held (W1) than the other (W2).

The Mn and Fe coordination octahedra are arranged in a corner-sharing fashion. Fe(II) and Mn(II) ions are on puckered sheets parallel to the *ab* plane where each metal ion is at the center of an approximately squared lattice defined by the other ion. The two sublattices are linked through nitroprusside equatorial cyanide ligands (Fig. 3).

Neighboring nitroprusside ions are antiparallel piled up along *b* with their NO groups eclipsed at the short distance of 3.77 Å. This arrangement gives rise to the relatively large Davydov splitting observed between the IR and Raman modes arising from the strongly polar NO stretching vibration.

The $\text{Mn}[\text{Fe}(\text{CN})_5\text{NO}]\cdot 2\text{H}_2\text{O}$ crystal and the corresponding trihydrated compound reported in ref. 2 are practically isomorphous. $\text{Mn}[\text{Fe}(\text{CN})_5\text{NO}]\cdot 3\text{H}_2\text{O}$ crystallizes in the monoclinic space group $P2_1/n$ with cell constants within 5% of the corresponding values for the dihydrated form. In fact, by interchanging the *a* and *b* unit cell vectors (and inverting *c*, to preserve a right-handed triad) defined in ref. 2, we obtain the space group setting $P2_1/n11$, subgroup of the $P2_1/n2_1/m2_1/a$ which corresponds to $\text{Mn}[\text{Fe}(\text{CN})_5\text{NO}]\cdot 2\text{H}_2\text{O}$. By applying the transformations $x_o=y_m, y_o=x_m, z_o=1/2-z_m$ to the atomic fractional coordinates

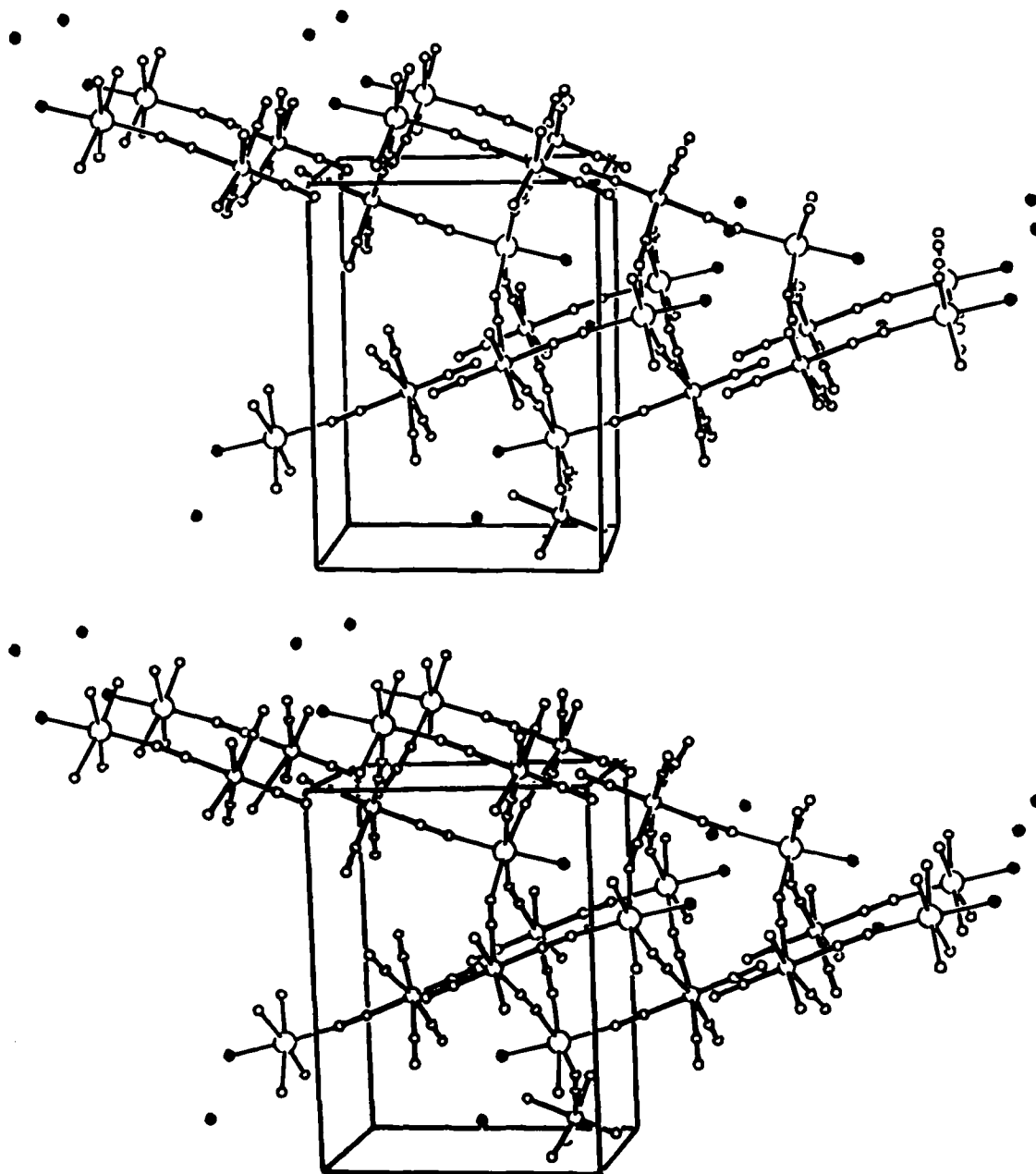


Fig. 3. A stereoscopic pair of a structure projection showing the crystal packing.

reported for the monoclinic $\text{Mn}[\text{Fe}(\text{CN})_5\text{NO}]\cdot 3\text{H}_2\text{O}$ crystal, we get approximate coordinates of the homologous atoms in orthorhombic $\text{Mn}[\text{Fe}(\text{CN})_5\text{NO}]\cdot 2\text{H}_2\text{O}$, with the only exception being the water oxygen labelled O(2) in the trihydrate. This is the water molecule which should be lost during the dehydration process: $\text{Mn}[\text{Fe}(\text{CN})_5\text{NO}]\cdot 3\text{H}_2\text{O}$ ($P2_1/n$) \rightarrow $\text{Mn}[\text{Fe}(\text{CN})_5\text{NO}]\cdot 2\text{H}_2\text{O}$ ($Pnma$). In this process, the $\text{Ow} \cdots \text{Ow}$ contact length of the pair of water oxygen atoms common to both hydrates reduces from 2.784(4)

to 2.587(9) Å. This suggests that the H-bond between the water molecules found in the dihydrate is stronger than the corresponding H-bond in the trihydrate crystal.

IR and Raman Spectra

Figure 4 displays room temperature IR and Raman spectra run at 1 and 2 cm^{-1} resolution, respec-

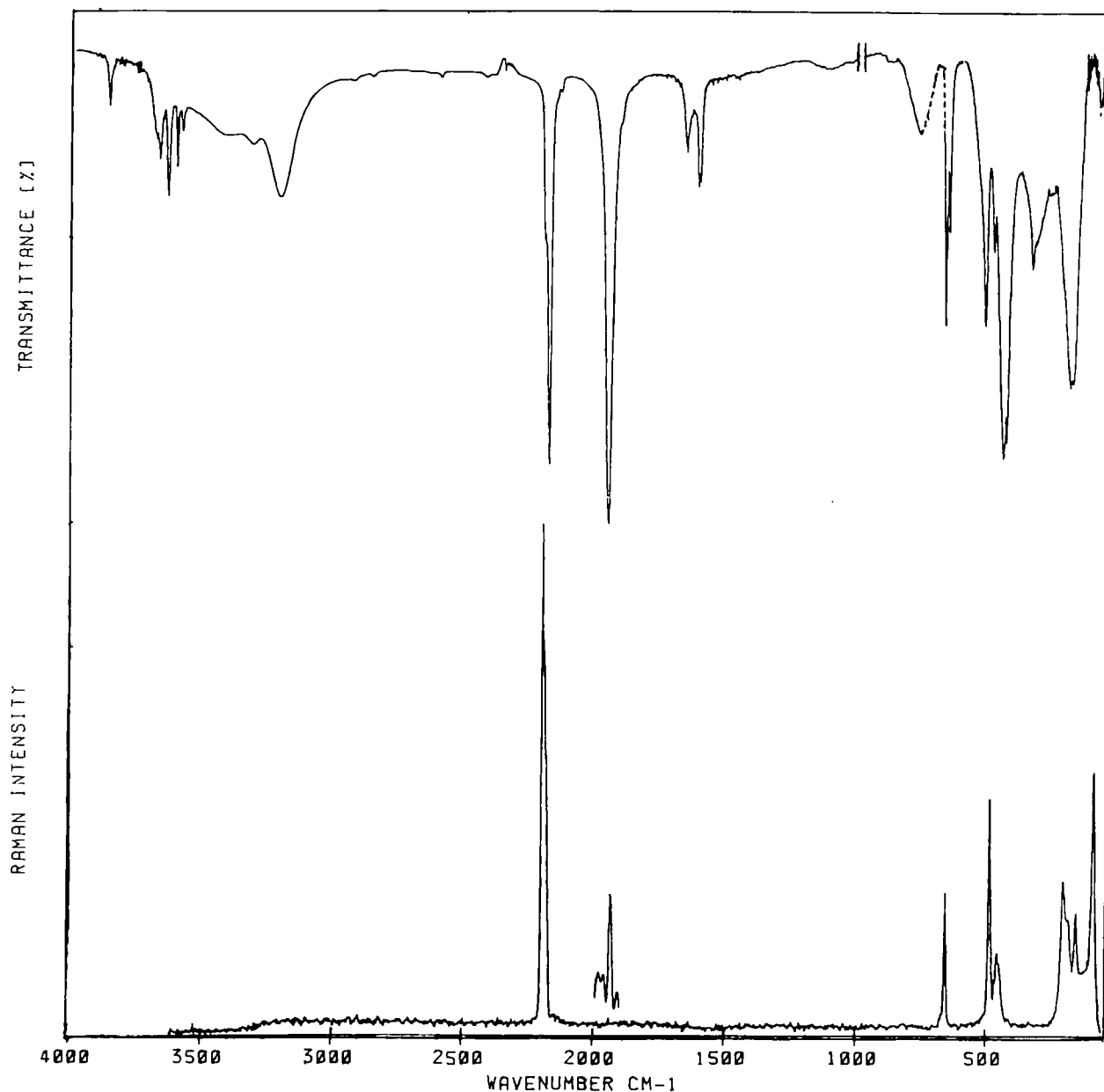


Fig. 4. FTIR and FTNIRR, room temperature, spectra, 1 and 2 cm^{-1} resolution, respectively. The insert in the Raman spectrum shows the NO stretching feature amplified.

tively. In the dashed IR region, polyethylene bands have been deleted (the spectrum sees as from KBr wafers). The insert in the Raman spectrum shows the νNO band intensified as a result of amplification of the signal obtained from 1500 spectral runs made to improve the signal-to-noise ratio. Table 4 presents FTIR and FTNIRR wavenumbers and assignments.

The IR spectrum of MnNP is representative of the spectra of one of the groups (group II) into which the first-series divalent transition- and post-transition

metal nitroprussides were divided based on their IR behavior.¹

Assignments follow a previous proposal¹ and recent assignments made for NaNP^{33d} (see refs. 33a-c for some other previous proposals); although for greater security in the assignments below 600 cm^{-1} a normal coordinate analysis should be performed as it was for NaNP^{33d} .

An extensive discussion¹ of IR bands due to the anion and to water points out the differences that distin-

Table 4. FTIR and FTNIRR (1 and 2 cm⁻¹ resolution, respectively) spectroscopic data and assignments

IR (cm ⁻¹)	Raman (cm ⁻¹)	Assignment ^a
3853		2νNO
3663		ν _{as} OH(W2)
3631		νOH(free)(W1)
3598		ν _{sym} OH(W2)
3578		?
ca. 3413		νO ₁ -H ··· O ₂
3313		
3201		
2194	2194	νCN _{ax} (A')
2188	2188	νCN _{eq} (A')
2180 sh	2180	νCN _{eq} (A'')
2175	ca. 2173 sh	νCN _{eq} (A' + A'')
1949	1939	νNO
1665		δW1
1606		δW2
784		LW1
665	664	δFeNO
652	651	νFeN
ca. 560 sh		LW2
ca. 535 sh		?
ca. 520 sh		δFeCN _{eq} (A')
513		δFeCN _{ax} (A' + A'')
ca. 505 sh		?
483	482	νFeC _{ax} (A')
	466	δFeCN _{eq} (A'')
	457	δFeCN _{eq} (A' + A'')
	ca. 448 sh	νFeC _{eq} (A'')?
443	ca. 441 sh	νFeC _{eq} (A' + A'')
	ca. 436 sh	νFeC _{eq} (A'')
430	ca. 429 sh	νFeC _{eq} (A')
339		δFeCN _{eq} (A' + A'')
323 sh		LW?
	ca. 207 sh	Lattice
	202	Lattice
	ca. 194 sh	Lattice?
190	ca. 189 sh	Lattice?
179	180	Lattice
	ca. 170 sh	Lattice?
	154	δC _{eq} FeN(A' + A'')
	ca. 134	δC _{eq} FeC _{ax} (A' + A'')
	ca. 122	δC _{eq} FeN + δC _{eq} FeC _{eq} (A' + A'')
	ca. 108 sh	Lattice?
	ca. 95 sh	Lattice?
84	86	δC _{eq} FeC _{eq} (A')
	ca. 75 sh	Lattice?

^a cf. ref. 33d.
sh: shoulder.

guish each type of spectrum, which is most evident in the case of water. The number and shapes of OH-stretching bands, and the existence of two bands due to angular deformations suggested the existence of two different types of water molecules with free or nearly

free (nonhydrogen bonded) OH groups, as well as a strongly H-bonded OH-group. The coordinated water (W1) is responsible for the very broad OH-stretching band which extends between 3550 and 3200 cm⁻¹ with a broad shoulder at about 3413 cm⁻¹ and peaking at 3313 and 3201 cm⁻¹. This is similar to the IR spectrum of hydrated Mn²⁺ with polystyrenesulphonate as counteranion (3406 ± 6 cm⁻¹).³⁴ The bending band as well as the librational band of highest wavenumbers (1655 and 784 cm⁻¹ broad, respectively) should also be assigned to this molecule. These three bands shift in the expected spectral directions (downwards, towards FIR, and upwards, towards NIR) and gain in intensity when cooling the sample.¹ Mullica *et al.*,² when discussing the water bands of the trihydrate, pointed to the existence of two types of hydrogen bonding, strong and weak (*sic*), and also stated that the hydrogen atoms of the coordinated (to cation) water molecule are responsible for the positioning of the uncoordinated water molecules within the channels that permeate the crystal lattice (*sic*). They reported that the features corresponding to the strongest bonded water molecule occur at 3210 (shoulder, broad), 1635 (shoulder), and 760 (shoulder, broad) cm⁻¹, respectively. These features turn into definite bands and are shifted in the correct spectral directions in the dihydrate spectrum which is expected from the weaker hydrogen bond existing in the trihydrate than in the dihydrate.

The free OH group of the water molecule (W1) of the dihydrate involved in the strong H-bonding gives rise to the strongest of all bands of the set of H-bonding-free OH groups which is located at 3631 cm⁻¹. This band is the first of the set to disappear in addition to the broad band characteristic of H-bonding (3550–3200 cm⁻¹), the bending band of highest wavenumber (1665 cm⁻¹) and the librational band also of highest wavenumber (784 cm⁻¹) upon controlled dehydration. The bands at 3663 and 3598 cm⁻¹ should be ascribed to the antisymmetric and the symmetric OH stretchings, respectively, of the least bonded water molecule (W2). These bands have wavenumbers even greater than the respective bands of the weak bonded water molecules of NaNP^{33a-d} (see ref. 33d for FTIR results, 3629.5 and 3546.6 cm⁻¹, respectively). The band of highest wavenumber of this set, located at 3663 cm⁻¹, and assigned to the antisymmetric OH stretching of W2, is only 3 cm⁻¹ below the highest wavenumber reported for Li₂[Fe(CN)₅NO]·2H₂O,⁶ considered as probably the highest ever reported for a hydrate and corresponding to a water molecule taken

as almost free.⁶ The sharp, very weak band at 3578 cm^{-1} remains unexplained.

To W2 should also be assigned the deformation band found at 1606 cm^{-1} and the shoulder at 560 cm^{-1} barely seen in the new spectrum but more noticeable at 530 cm^{-1} in the low-temperature spectrum.¹ In the room temperature NaNP spectrum, these features appear at 1618 and 522 cm^{-1} , respectively.^{33†} The sharp, very weak band at 3578 cm^{-1} remains unexplained.

The very strong IR CN stretching band assigned to the E (under ideal C_{4v} symmetry for the anion but $A' + A''$ under real, C_s symmetry) stretchings of the equatorial groups is located at 2175 cm^{-1} , 31 cm^{-1} higher than the corresponding band of NaNP which appears at 2144 cm^{-1} .^{33d} This increase in wavenumber is the result of the bonding of the CN groups (through the N atoms) to the cation, Mn^{2+} . The NO stretching band wavenumber (1949 cm^{-1}) is also greater (5 cm^{-1}) than in NaNP spectrum^{33d} due to the bonding of the cyanides to Mn^{2+} which favors the back donation of electron charge to these groups and, consequently, disfavors the $d_{\pi}(\text{Fe}) \rightarrow \pi^*(\text{NO})$ back-bonding leading to an increase in νNO .

The vibrational coupling existing between the antiparallel, closely packed NO groups could also behave in a similar manner.

The δFeNO and νFeN wavenumbers (665 and 652 cm^{-1} , respectively) are similar to the corresponding values in NaNP (663 and 652 cm^{-1} , respectively) due to the fact that the NO groups are not coordinated and the vibrational coupling does not affect these bands.²⁶

The low wavenumber bands (below 500 cm^{-1}) are also NIR shifted for the same reason. Assignments in this spectral region should be complicated because bands due to the anion, water, and core MnN_5O are found.^{35a,b} In fact, only one band, at 339 cm^{-1} , is found which is assigned to an internal nitroprusside mode by comparison with NaNP.^{33d}

The Raman spectrum is simplified by the lack of water bands and looks very much like the NaNP spectrum. As stated above, the IR νNO band is located at 1949 cm^{-1} , i.e., 10 cm^{-1} above the Raman value (1939 cm^{-1}), a difference which should be ascribed to a strong vibrational coupling between neighboring, antiparallel NO groups. For barium nitroprusside trihydrate, where a strong vibrational coupling was previously recognized,²⁶ the difference is 11 cm^{-1} ^{26,27} while in sodium nitroprusside dihydrate,³⁶ where such a strong coupling does not exist, it is -6.7 cm^{-1} , i.e., the Raman band wavenumber is greater than the IR

value.^{33d} The most intense CN stretching Raman band which is assigned to the axial (along the slightly broken line: NCFeNO), $A_1 (A')$ mode is located at 2194 cm^{-1} , the same value as in the IR spectrum, while in the NaNP spectrum it appears 20 cm^{-1} below, this difference is due to the coordination of the CN axial groups with Mn^{2+} .

Conclusions

Single crystals of manganese(II) nitroprusside formed by double decomposition between slowly inter-diffusing reactants proved to be a dihydrate when examined using X-ray crystallographic analysis. When dried in the air or kept under absolute ethanol the hydrate composition remained but further drying results first in the formation of the monohydrate and finally, the anhydrate. The crystals of the dihydrate are topotactically related to those of the trihydrate.² In the dihydrate, anions are arranged in double chains and the NO groups are antiparallel intercalated, at the short, 3.7 \AA distance between neighbors. This arrangement brings about a strong vibrational coupling between the NO groups which manifests as a $+10 \text{ cm}^{-1}$ difference between the stretching IR and Raman wavenumbers. One of the water molecules (W1) is coordinated to the Mn^{2+} ion which completes its coordination octahedron with five N atoms and is strongly H(as donor)-bonded to the other water molecule (W2), forming a linear and very short bond. The other hydrogen atom of W1 and the hydrogen atoms of W2 seem to be free or nearly free from H-bonds.

The IR spectrum shows, as distinct details, bands due to the tightly bonded water molecule W1 but in other aspects the spectrum looks very much alike NaNP spectrum but NIR shifted due to the coordination of the N(C) atoms with the cation. The same is true for the Raman spectrum, which looks obviously simpler than the IR spectrum due to negligible Raman activity of water and the very poor Raman response of the NO group which is due in both cases to the low polarizabilities of these components.

TGA results confirm the dihydrate character of the compound and the presence of the two differently bonded water molecules. Controlled dehydration leads in the first step, to a monohydrate.

Note

After sending the manuscript to publication our attention was called to the paper of E. Reguera, A.

Dago, A. Gómez, and J. F. Beltrán, *Polyhedron* **1996**, *15*, 3139 where the orthorhombic unit cell $Pnma$ ($a = 14.112(6)$, $b = 7.511(3)$, $c = 10.542(3)$, $Z = 4$), deduced from powder X-ray diffractograms, is also proposed for $Mn[Fe(CN)_5NO] \cdot 2H_2O$. It is stated there that crystals of $Mn[Fe(CN)_5NO] \cdot 3H_2O$, grown using the 'slow diffusion tube' method, dehydrate to the dihydrate when exposed to the atmosphere and become brittle producing a polycrystalline material.

Thanks are due to the referee and to the Editor for helpful suggestions to improve the manuscript.

Acknowledgments

To Consejo Nacional de Investigaciones Científicas y Técnicas (CONICET), Argentina, for financial support to CEQUINOR and PROFIMO. To Comisión de Investigaciones Científicas de la Provincia de Buenos Aires (CICPBA), Argentina, for the same kind of support to CEQUINOR. To Universidad Nacional de La Plata, Argentina, for a research grant to P.J.A. To Conselho Nacional de Pesquisas (CNPq), Fundação de Amparo e Pesquisa do Estado de São Paulo (FAPESP), Financiadora de Estudos e Projetos (FINEP) and Fundação Vitae, Brazil, for financial help to O.E.P. and E.E.

Supplementary material. Crystallographic data (excluding structure factors) for the structure reported in this paper have been deposited with the Cambridge Crystallographic Data Centre as supplementary publication no. CCDC-1003/5179. Copies of available material can be obtained, free of charge, on application to the Director, CCDC, 12 Union Road, Cambridge CB2 1EZ, UK, (fax: +44-(0)1223-336033 or e-mail: teched@chemcryst.cam.ac.uk).

References

- Gentil, L.A.; Baran, E.J.; Aymonino, P.J. *Inorg. Chim. Acta* **1976**, *20*, 251.
- Mullica, D.F.; Tippin, D.B.; Sappenfield, E. *Inorg. Chim. Acta* **1990**, *174*, 129.
- Castellano, E.E.; Piro, O.E.; Rivero, B.E. *Acta Crystallogr.* **1977**, *B33*, 1725.
- Castellano, E.E.; Piro, O.E.; Podjarny, A.D.; Rivero, B.E.; Aymonino, P.J.; Lesk, J.H.; Varette, E.L. *Acta Crystallogr.* **1976**, *B34*, 2673.
- Della Védova, C.O.; Lesk, J.H.; Varette, E.L.; Aymonino, P.J.; Piro, O.E.; Rivero, B.E.; Castellano, E.E. *J. Mol. Struct.* **1961**, *70*, 241.
- Vergara, M.; Varette, E.L. *Spectrochim. Acta* **1993**, *49A*, 527.
- Retzlaff, C. *PhD Thesis*; Köln University: Germany, 1987.
- Le Page, Y.; Castellano, E.E. *Acta Crystallogr.* **1990**, *C46*, 1577.
- Amalvy, J.I.; Varette, E.L.; Aymonino, P.J.; Castellano, E.E.; Piro, O.E.; Punte, G. *J. Crystallogr. Spectrosc. Res.* **1986**, *16*, 537.
- Amalvy, J.I.; Varette, E.L.; Aymonino, P.J. *J. Phys. Chem. Solids* **1985**, *46*, 1153.
- Castellano, E.E.; Rivero, B.E.; Piro, O.E.; Amalvy, J.I.; Aymonino, P.J. *Acta Crystallogr.* **1989**, *C45*, 1207.
- Soria, D.B.; Amalvy, J.I.; Piro, O.E.; Castellano, E.E.; Aymonino, P.J. *J. Chem. Crystallogr.* **1996**, *26*, 325.
- Soria, D.B.; Amalvy, J.I.; Piro, O.E.; Castellano, E.E.; Aymonino, P.J. *X Argentinian Physical Chemistry Congress*; S.M. de Tucumán: Argentina; April 21–25, 1997 (to be published elsewhere).
- Vergara, M.; Varette, E.L.; Rigotti, G.; Navaza, A. *J. Phys. Chem. Solids* **1989**, *50*, 951.
- Vergara, M.; Varette, E.L. *J. Phys. Chem. Solids* **1987**, *48*, 13.
- Rigotti, G.; Aymonino, P.J.; Varette, E.L. *J. Crystallogr. Spectrosc. Res.* **1984**, *14*, 517.
- Punte, G.; Rigotti, G.; Rivero, B.E.; Podjarny, A.D.; Castellano, E.E. *Acta Crystallogr.* **1980**, *B36*, 1472.
- Retzlaff, C.; Krumbe, W.; Dörfel, M.; Haussühl, S. *Z. Crystallogr.* **1989**, *189*, 141.
- Navaza, A.; Chevrier, G.; Güida, J.A. *J. Solid State Chem.* **1995**, *114*, 102.
- Hauser, U.; Oestreich, V.; Rohrweck, H.D. *Z. Phys.* **1977**, *A280*, 17, 125; *Phys.* **1978**, *A284*, 9.
- Güida, J.A.; Piro, O.E.; Aymonino, P.J. *Solid State Comm.* **1986**, *57*, 175.
- Güida, J.A.; Piro, O.E.; Aymonino, P.J. *Solid State Comm.* **1988**, *66*, 1007.
- Zöllner, H.; Krasser, W.; Woike, Th.; Haussühl, S. *Chem. Phys. Lett.* **1989**, *161*, 497.
- (a) Güida, J.A.; Piro, O.E.; Shaiquevich, P.; Aymonino, P.J. *Solid State Comm.* **1997**, *101*, 471; (b) Güida, J.A.; Piro, O.E.; Aymonino, P.J. *Inorg. Chem.* **1995**, *34*, 4113.
- Varette, E.L.; Aymonino, P.J. *Inorg. Chim. Acta* **1973**, *7*, 597.
- González, S.R.; Aymonino, P.J.; Piro, O.E. *J. Chem. Phys.* **1984**, *81*, 625; González, S.R.; Piro, O.E.; Aymonino, P.J.; Castellano, E.E. *Phys. Rev. B15*; González, S.R.; Piro, O.E., Aymonino, P.J.; Castellano, E.E. *Phys. Rev. B15*; **1986**, *33*, 5818.
- Güida, J.A.; Piro, O.E.; Aymonino, P.J.; Sala, O. *J. Raman Spectrosc.* **1992**, *23*, 131.
- Chamberlain, M.M.; Green, A.F. Jr. *J. Inorg. Nucl. Chem.* **1963**, *25*, 1471.
- Sheldrick, G.M. *Acta Crystallogr.* **1990**, *A46*, 467.
- Sheldrick, G.M. *SHELXL93, a Program for Crystal Structure Refinement*; University of Göttingen: Germany, 1993.
- Hamilton, W.C. *Acta Crystallogr.* **1959**, *12*, 609.
- Johnson, C.K. *ORTEP, Report ORNL-3794*; Oak Ridge, TN., 1965.
- (a) Khanna, R.K.; Brown, C.W.; Jones, L.H. *Inorg. Chem.* **1969**, *8*, 2195; (b) Bates, J.B.; Khanna, R.K. *Inorg. Chem.* **1970**, *9*, 1376; (c) Zhakariev, O.; Woike, Th.; Haussühl, S. *Spectrochim. Acta* **1995**, *51A*, 447; (d) Chacón Villalba, M.E. *Doctoral Thesis*: Universidad Nacional de La Plata: La Plata, Argentina, 1995; Chacón Villalba, M.E.; Varette, E.L.; Aymonino, P.J., *Vibrat. Spectrosc.*, Part I accepted; Part II sent for publication.
- Zundel, G.; Murr, A. *Z. Physik. Chem. N.F.* **1976**, *54*, 59.
- (a) Nakamoto, K. *Infrared and Raman Spectra of Inorganic and Coordination Compounds*; 4th Edition, Wiley: New York, 1986; (b) Weidlein, J.; Müller, U.; Dehnicke, K. *Schwingungsfrequenzen II, Nebengruppenelemente*; Georg Thieme Verlag: Stuttgart, Germany, 1986.
- Bottomley, F.; White, P.S. *Acta Crystallogr.* **1979**, *B35*, 2193.